Journal of Archaeological Science: Reports 33 (2020) 102568

Contents lists available at ScienceDirect

Journal of Archaeological Science: Reports

journal homepage: www.elsevier.com/locate/jasrep

Identifying metallurgical practices at a colonial silver refinery in Puno, Peru, using portable X-Ray fluorescence spectroscopy (pXRF)

Sarah A. Kennedy[a,*], Sarah J. Kelloway[b]

[a] Department of Anthropology, University of Pittsburgh, 3302 WWPH, Pittsburgh, PA 15260, USA
[b] Sydney Analytical, University of Sydney, Madsen Building, Camperdown, NSW 2006, Australia

ARTICLE INFO

Keywords:
Andes
Colonial
pXRF
Silver refining
Patio process
Mercury amalgamation
High-altitude

ABSTRACT

This study presents the results of *in situ* portable X-ray fluorescence (pXRF) analyses of surface soils at the site of Trapiche Itapalluni, a Spanish colonial silver refinery located 15 km southwest of Puno, Peru in the western Lake Titicaca Basin (4000 masl). Although the benefits of pXRF analysis are well known, such as its wide availability and rapid, non-destructive nature, there has been little applicability of this technique at colonial metallurgical sites in the high-altitude Andes. The results of our analysis confirmed the introduction of the patio process technique of silver refining from Mexico to the Puno Bay, and further clarified areas of intense metallurgical production, including local Andean adaptations. This study highlights the advantages of *in situ* pXRF analysis of surface soils at industrial archaeology sites, especially in marginal and high-altitude environments such as the southern Andes.

1. Introduction

Field portable X-ray fluorescence (pXRF) spectroscopy has been increasingly used for preliminary geophysical site surveys of surface soils in metallurgical and historical contexts (Booth et al., 2017; Coronel et al., 2014; Frahm et al., 2016; Hanks, 2013; Hayes, 2013; Kincey et al., 2018; Lubos et al., 2016; Scott et al., 2016; Tighe et al., 2018). Such pXRF soil surveys have been especially valuable where a given metallurgical activity is associated with a specific element, essentially providing a diagnostic elemental marker in the soil (Millard, 1999; Jones, 2001; MacKenzie and Pulford, 2002; White and Dungworth, 2007). In addition to reconstructing past metallurgical practices, this type of analysis also has the potential to inform day-to-day objectives and decisions in the field by facilitating real-time data processing.

One area of the world where the use of pXRF analysis in ancient metallurgical contexts could be particularly useful is the south-central Andes of Peru, where mining, smelting, and refining has had a long history. The south-central Andes were a key location for the development of early indigenous silver smelting technology (Abbott and Wolfe, 2003; Cooke et al., 2008; Schultze, 2013) and following the Spanish conquest in 1532 CE, Andean mineral resources became critical to the Spanish economy, especially silver, whose complex geological makeup made it more difficult to extract than other precious metals. Silver is usually found in a combined state in nature, within lead, iron, and copper ore (Guerrero, 2017), and in the Andes, most deep silver deposits were composites of silver sulfide ores (called *negrillos*). During the 1570s, a complex method of mercury amalgamation with copper sulfate called the patio process (*beneficio de patio* in Spanish) was brought to the Andes from Mexico. Through this complex process, laborers were able to derive pure silver from silver sulfide ores at refineries.

This paper presents the results of a pXRF soil survey conducted at one of these colonial silver refineries, Trapiche Itapalluni ("Trapiche"), located 15 km southwest of Puno, Peru, in the western Lake Titicaca Basin (1650–1800 CE) (Fig. 1). pXRF results were used to identify metallurgical activity areas at the site, clarifying the location and stages of the patio process at Trapiche. High levels of mercury (Hg) were identified in two main locations, establishing the location of multiple stages of silver refining, including mercury amalgamation. High levels of copper (Cu) and iron (Fe) were associated with roasting and heating practices, revealing local Andean adaptations to the patio process. While there was initial concern about the functionality of pXRF in high-altitude, marginal environments, the instrument functioned well with only some elemental concentrations affected by altitude.

2. Using pXRF for geochemical soil surface survey: advantages and limitations

The introduction of pXRF technology has had a significant impact

* Corresponding author.
E-mail addresses: sak201@pitt.edu (S.A. Kennedy), sarah.kelloway@sydney.edu.au (S.J. Kelloway).

https://doi.org/10.1016/j.jasrep.2020.102568
Received 12 February 2020; Received in revised form 1 September 2020; Accepted 2 September 2020

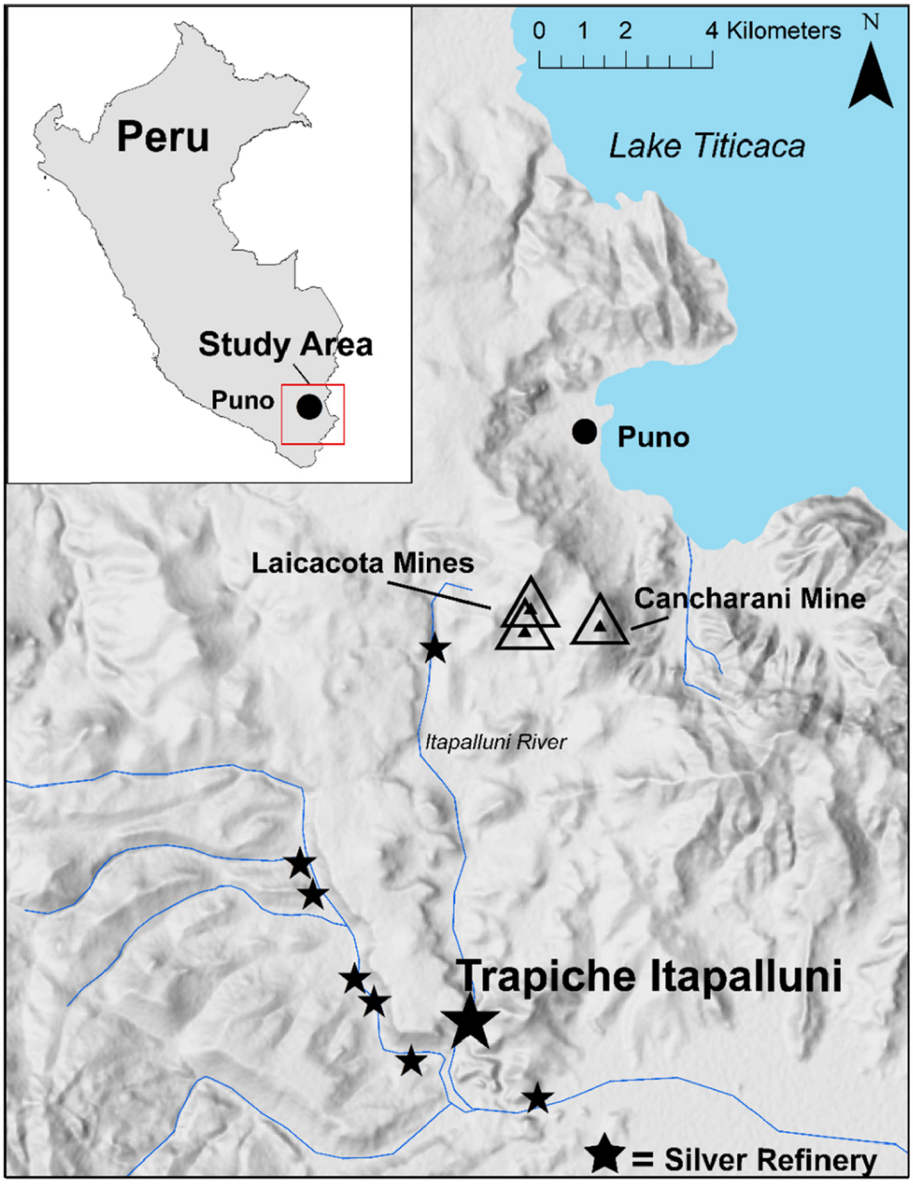

Fig. 1. Map of the study location, Trapiche Itapalluni, in the Puno Bay of southern Peru shown in relation to other colonial silver refineries and mines.

on archaeology, soil science, and public health over the past two decades. Originally developed for mineral and mining research, the many advantages of pXRF spectrometers, notably their high portability, potential for non-destructive analyses, relatively low cost, and commercial availability, have since made them a powerful tool across a variety of fields. The most successful of these studies have also considered the limitations of this technique (Malainey, 2011). Recent archeometallurgical studies have seen especially promising results using pXRF to identify and assess copper levels in soils at ancient mining sites (Rogan et al., 2019; Shalev et al., 2006; Tighe et al., 2018).

Methodological issues related to pXRF technology within the field of archaeology have been widely detailed over the last decade (Aimers et al., 2012; Hunt and Speakman, 2015; Killick, 2015; Shackley, 2010, 2011; Speakman et al., 2011; Speakman and Shackley, 2013). Many archaeological studies have used pXRF analyses to chemically characterize obsidian, metal, and ceramics. As our present study focusses on the identification of heavy metals in soils, we summarize issues related to soil-based pXRF studies below.

A major issue affecting pXRF analyses of soils in the field is the environment. Altitude, soil moisture, and soil matrix all affect pXRF readings. High altitude has been shown to affect pXRF instruments, resulting in higher concentration readings of certain elements at higher altitudes, or total malfunction of the instrument due to internal condensation and unequal air pressure (Merrill et al., 2018). These effects are particularly important when considering work in the high-altitude Andes. Studies have shown that pXRF instruments without built-in pressure corrections will overreport levels of low-atomic weight elements, such as sodium, magnesium, aluminum, silicon, phosphorus, sulfur, chlorine, potassium, and calcium (Malainey, 2011; Merrill et al., 2018). In turn, this may result in the pXRF instrument under-reporting heavy elements (e.g., lead, mercury), and even where correction systems are in place, a check sample should be run at both low and high-altitudes to identify any such problems with concentration data.

Soil moisture can also affect pXRF readings, with moisture changes occurring over the course of a day, as well as over multiple days (Padilla et al., 2019). Further, *in situ,* un-prepared soil samples will not be homogenous, and differences in the presence of roots, stones, and compactness, for example, can lead to high sample variability and variations in measurements, particularly in relation to light elements.

3. Silver smelting, mercury amalgamation, and the patio process

3.1. The early colonial silver production system

Prior to the introduction of the patio process to the Andes in the 1570s, silver was extracted from ore through smelting. This occurred using indigenous technology called *huayrachinas* (wind or draft furnaces) and *tocochimbos* (cupellation hearths). *Huayrachinas* were used to heat pulverized silver ore, which was mixed with a lead sulfide. Upon heating, the lead and silver combined. The lead/silver bullion was further refined in a *tocochimbo,* a small cupellation hearth used with a blow pipe, to remove the lead and leave pure silver (Van Buren and Mills, 2005). The scale of production with indigenous technology was relatively small, as the furnaces and hearths could not be increased in size without losing their functionality (Van Buren and Cohen, 2010). By the 1560s, the easily smelted silver ores from superficial and weathered deposits (*colorados*) were mined out, leaving the harder to process, deeper silver sulfide ores (*negrillos*) (Guerrero, 2016:6; Guerrero, 2017:101).

The inability to extract silver from deeper deposits was a problem for the Spanish government, which relied heavily on the colonial silver mining economy for revenue. Fortuitously, an alternative to smelting called mercury amalgamation was discovered in Venice in the mid-16th century. This new process did not need high temperatures to extract silver, offsetting much of the cost of charcoal fuel (Guerrero, 2017:101). Through a series of chemical reactions, mercury was mixed with crushed silver ore to form a bonded alloy, or amalgam, of mercury and silver. The mercury/silver amalgam was then heated, which removed the mercury through evaporation, leaving pure silver (Guerrero, 2017:55, 102-103).

Following the discovery of mercury amalgamation, Spain quickly brought the technology to the Americas. Aided by German and indigenous refiners, Bartolomé de Medina is credited with the first use of mercury amalgamation on American ores in Mexico in 1556 (Bargalló, 1969; Bigelow, 2020). However, the silver sulfide *negrillos* still proved challenging to refine until Medina discovered that adding a copper sulfate (the *magistral*) made refining possible (Bargalló, 1966, 1969; Guerrero, 2016:7). When silver sulfide is combined with copper in a saline solution, it produces silver chloride (AgCl), which can be broken down to elemental silver when it reacts with mercury (Fig. 2) (Guerrero, 2017).

Medina's technique (patio process) was complex and included many steps: grinding, drying and salting the ore; mixing it with mercury and the *magistral*; leaving it to sit in the sun; washing it to remove the mercury/silver amalgam; evaporating mercury from the amalgam; heating the silver to remove any last impurities; and finally forming it into bars (Bargalló, 1966; Bigelow, 2020). In Mexico, the only part of the process that involved heat was the last steps. Otherwise, sunlight was the only heat source. The process took place in large patios and courtyards, hence the name patio process (Guerrero, 2017:103).

Often lost in the discussion of the patio process is how local refiners adapted refining techniques *in situ* (Bigelow, 2020; Guerrero, 2016). When Medina's patio process was brought to the Andes by Fernández de Velasco in 1572, it was initially challenging to replicate due to the high altitude, cold weather, and marginal environment. Heat from the sun was not sufficient to initiate the necessary chemical reactions, and wood, charcoal, and dried llama dung were needed as fuel to add heat to the process. To offset costs, Andean refiners discovered that roasting silver sulfide ores with salt at the beginning of the process converted the ore to silver chloride without using the *magistral* (Barba, 1640). Iron and copper were also discovered to reduce silver chloride to elemental silver without adding mercury. These Andean developments (Fig. 2) reduced the amount of costly mercury needed for the patio process (Guerrero, 2017:121).

3.2. Silver refineries, architectural layout, and pXRF analysis

Although a technological advancement, the patio process did have its drawbacks, specifically the large increase of labor and materials necessary to refine silver. The new process required additional miners, and the extracted ores needed to be transported to refineries. Further, the refineries needed to be constructed near water sources large enough to power grinding mills. A large supply of men and women were needed to work in the refineries themselves. A further drawback of this process was the negative health effects workers and their families faced due to inhalation of mercury vapor and dust (Robins, 2011; Robins and Hagan, 2012).

Silver ore was processed at both *trapiches* (small grist mills) and *ingenios* (stamp mills with large stamp heads) (Galaor, 1998:144). Once the ore was ground into a flour-like consistency, it was roasted with salt in reverberatory furnaces. The mixture was then placed in mixing containers (*buitrones*) in open-air patios. Salt, the *magistral*, and mercury were added to the *buitrones* and the mixture was left to sit in the sun to form the mercury/silver amalgam (*pella*). Heat and mercury were added, and laborers walked upon the mixture with their bare feet, to encourage the amalgamation process. Once the amalgam (*pella*) was formed, the mixture was taken to watertight tanks (*potros*). Laborers again agitated the mixture with their feet, and the heavy *pellas* sank to the bottom and were collected. Extra mercury was squeezed out of the *pellas,* which were then placed in pineapple-shaped molds and heated, where the mercury evaporated, leaving behind pure silver (*piñas)* (Galaor, 1998:144–145). The latter stages of the process were especially dangerous for refinery laborers, as they were continuously exposed to liquid and vaporized mercury (Robins, 2011).

Because the silver refining process had to be carried out in specific stages at specific locations, activity areas within refineries are identifiable. Architectural elements, such as grinding stones, ovens, and water tanks, can be combined with soil pXRF analyses to further identify metallurgical areas. In this study, we use pXRF to identify the presence of mercury at Trapiche to confirm the use of the patio process. Additionally, we use pXRF analysis to assess if roasting, a *magistral* process, or both, were used to refine silver ore.

4. The Puno Bay

4.1. Laicacota and Cancharani

Our study took place in the Puno Bay, located in the western Lake Titicaca Basin of Peru. The Puno Bay was a key location for the development of early indigenous silver smelting and was an area of metallurgical importance during Inka and Spanish colonization (Abbott and Wolfe, 2003; Cooke et al., 2008; Schultze, 2013). Although the silver rush of Potosí overshadowed the mineral potential of the Puno region for a time, the discovery of silver ore at the Laicacota mine in 1657 initiated a boom in silver production for many decades (Schultze, 2013).

The Laicacota mine is located in Tertiary Sillapata volcanic formation within porphyry copper deposits (ESDAC, 2020; Schultze, 2008:24-27; USGS, 2020). Modern mining reports detail the presence of lead, zinc, and silver at Laicacota (see Fig. 1) (USGS, 2020). Other ores and minerals at Laicacota include galena, sphalerite, barite, calcite, pyrite, and quartz. The late 20th century reports state that Laicacota silver was found in galena deposits, likely argentiferous galena (PbS with Ag). It is unclear if the 17th century ore deposits were also argentiferous galena, and we are unable to rule out the use of silver sulfide compounds and other halides (Guerrero, 2016:5-6).

The first silver boom at Laicacota lasted between 1657 and 1670 and corresponded to a period of unrest known as the Laicacota Conflict. Spanish Andalusian and Basque factions continuously fought for the

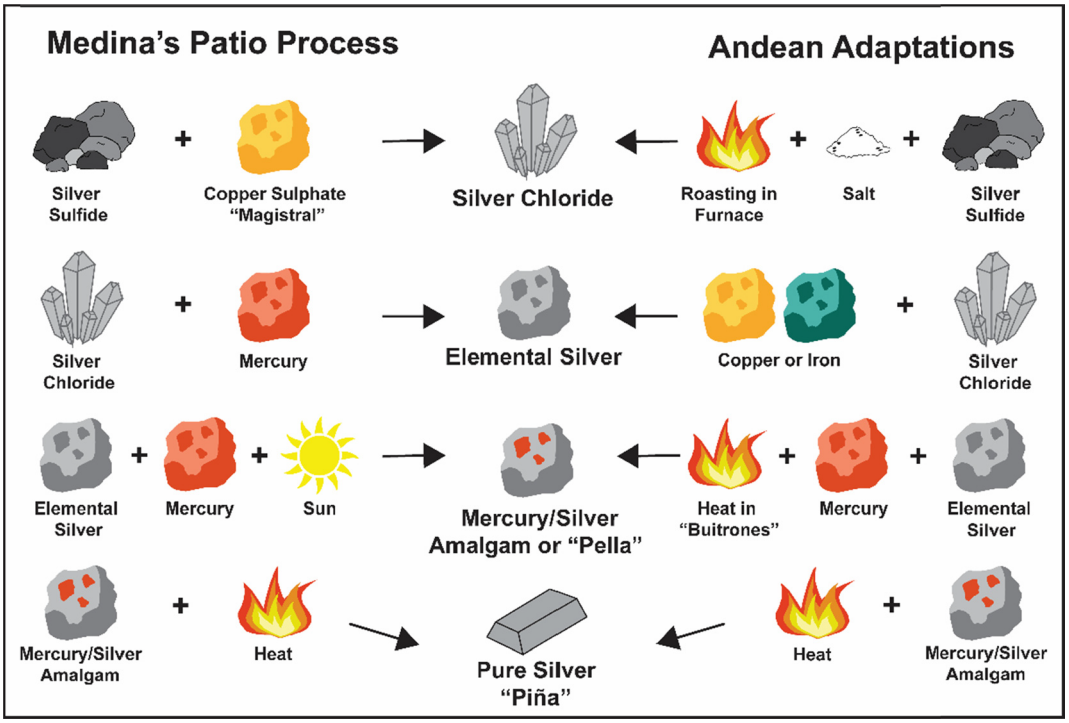

Fig. 2. Visual representation of the patio process, with Medina's original Mexican process illustrated at left, and Andean adaptations to the process illustrated at right.

control of the Puno mines, which reduced silver production in the area (Dodge, 1984; Dominguez, 2006). By the 1670s and 1680s, Laicacota silver mine operations were halted due to infrequent maintenance, resulting in mine flooding (Cañete y Domínguez, 1952[1791]:650; Galaor, 1998:134). The Puno Bay saw a second resurgence in silver mining in 1744 at the Cancharani mine adjacent to Laicacota, which lasted until the end of the 18th century. During this period, the Laicacota Conflict in the Puno Bay had ended, and many laborers eagerly came to work at the mines. A 1753 mining report details over sixty indigenous laborers working at a single silver refinery in the area. Described as *indios voluntarios* (volunteers), these workers were indigenous men and women drawn to the Puno Bay for increased economic opportunity, despite the known dangers of working in silver refineries (Galaor, 1998:146).

4.2. Trapiche Itapalluni

Our present study concentrated on one Puno Bay silver refinery, Trapiche, located 12 km southwest of Puno. The site encompasses 6000 m^2 and includes the remains of a large mill, thirty stone structures, a large work patio, and one midden. We have been unable to locate definitive documents as to the original name and ownership of Trapiche, and base many of our interpretations on documents that describe adjacent refineries. We estimate the site was occupied between 1660 and 1800 due to architectural style and presence of diagnostic artifacts, such as beads and coins. Radiocarbon dating confirms this period of use and indicates that Trapiche likely processed ore from both the Laicacota and Cancharani mines. The pXRF survey took place within the architectural core of Trapiche, which includes three main sectors (Fig. 3). Sector A is the northern-most sector, housing the mill, as well as seven smaller structures measuring approximately 3 m × 2.5 m, presumably used as residences for workers and for storage. Sector B is the middle and largest sector and functioned as a metallurgical and administrative zone. It includes the remains of a large reverberatory furnace, a metallurgical oven, cisterns, and the main work patio. It also includes a mixture of residential and storage structures. Sector C constitutes the southernmost sector and likely served as the principal entrance to the site. It includes a midden, residential structures, and a large multi-function building measuring 6.5 m × 4.5 m. Sector C also includes an open area directly north of the multiple-function building.

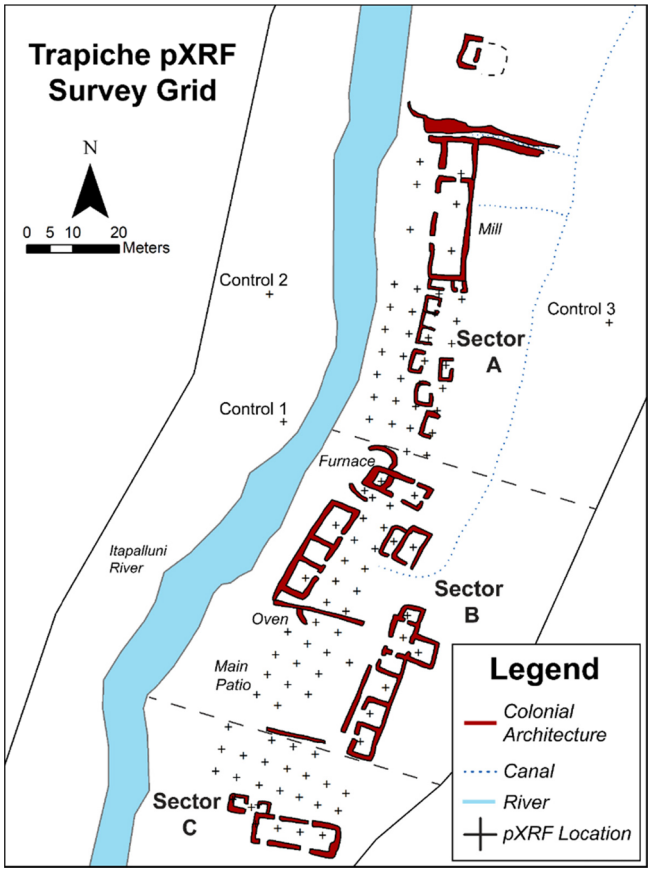

Fig. 3. Trapiche's architectural core, with pXRF survey locations.

5. Methodology

5.1. Survey methods

We established a survey grid across the site of Trapiche, with *in situ* pXRF analyses occurring at 5 m intervals. We concentrated the survey within Sectors A, B, and C and the analyses were taken from within buildings and patios. Each sampling location was recorded using a total station. Prior to analysis, each survey point was cleared of 3–5 cm of surface debris and photographed. Roots and pebbles were avoided for analysis, with the scraped earth visually checked and cleared before analysis. A polypropylene film was placed over the sample area before placing the window of the pXRF on the analysis spot to ensure the pXRF window was kept clean. The film was cleaned with a microfiber cloth between each sample location.

In total, we analyzed 100 sample spots from Trapiche, with three additional control locations taken outside of the site boundary, for a total of 103 readings. The pXRF survey took three days, for an average of 34 samples per day. Each night, the data was downloaded from the pXRF instrument and stored electronically. Output was in ppm. The results of the pXRF survey were available immediately and were used to make real-time decisions during excavation.

5.2. pXRF setup

The field survey was conducted using an Olympus Delta Premium (model DP-6000-C) portable XRF spectrometer, equipped with a Rh-anode tube and borrowed from the Mark Wainwright Analytical Centre (MWAC), University of New South Wales. The factory-set Soil Mode was selected as the initial basis for the work program covering the following elements: P, S, Cl, K, Ca, Ti, V, Cr, Mn, Fe, Co, Ni, Cu, Zn, As, Se, Rb, Sr, Y, Zr, Nb, Mo, Ag, Cd, Sn, Sb, W, Hg, Pb, Bi, Th, and U. Soil Mode operates three beams at various voltage, current, and filter settings, using a Compton normalization method for calibration: beam 1 at 40 kV, 72 μA (150 μm Cu filter); beam 2 at 40 kV, 73 μA (2 mm Al filter); and beam 3 at 15 kV, 132 μA (100 μm Al filter). Each mode was run for 30 seconds live time and the total area of the spot analyzed by the instrument was an ellipse approximately 8 mm by 10 mm. A standard was run daily to check for changes that might affect readings.

5.3. Factor correction

Field results indicated certain element values were beyond the factory Soil Mode calibration range. As such, representative survey points were sampled and the soils sent to the XRF Laboratory, MWAC, for analysis and use as standards for factor correction of the Soil Mode program. These soil samples were passed through a 500 μm sieve and split into quarters using a riffle splitter. A quarter of each sample was ground in a tungsten carbide mill for 90 seconds, with the remainder kept aside for other analyses. Subsamples of the ground material were analyzed by laboratory-based XRF using a PANalytical Axios Advanced WD-XRF spectrometer, equipped with a Rh tube. Pellets were made for trace element analysis by the Protrace program and in the case of Hg, a selection of samples representative of the concentration range covered were submitted for ICP-MS analysis. Glass beads were made for major element analysis, which were measured using a WROXI-based program. These major and trace results formed the expected standard concentrations for any required factor-correction. Another subsample of ground soil was analyzed on the pXRF spectrometer in cups using polypropylene film, and these values then formed the observed values to be used in correction.

To determine if factor corrections were indeed needed, the observed values to be used in correction were plotted against the WD-XRF laboratory results/expected results, using Microsoft Excel. A review of each element was performed, and the relative errors were calculated for the samples. Some elements were immediately excluded from analysis: Co and W were potential contaminants from grinding the subsamples; Ti, V, Zn, Rb, Sr, Y, Zr, Nb, and Th were not considered significant to the patio process and were excluded; Cl was excluded, as no values were determined by WD-XRF and so correction could not take place; Ni, Se, Mo, Cd, Sn, Bi, and U were excluded as many pXRF and WD-XRF results were below levels of detection and not enough samples had values above levels of detection to make a plot for correction. High relative errors and high levels of detection also meant the exclusion of P and Cr. The review also showed that some elements did not require correction (K, Ca, and Cu) and some only needed corrections where concentrations were above a threshold determined by inspecting plots and relative errors (Fe levels over 10,000 ppm; Pb levels over 1000 ppm; Hg values over 100 ppm). For S, separate factor corrections were needed for samples with high Fe, S, and Pb.

Where a correction was required, a factor was then applied to Soil Mode based on the linear equation resulting from the plot of the observed pXRF and WD-XRF values of the subsampled soils. The accuracy and precision of the corrected pXRF subsoil data was determined by comparing the data with the corresponding WD-XRF concentrations for samples that had been purposely excluded from factor correction work. Checks suggest that one could consider the level of determination for Ag and Sb to be ~ 20 ppm. Once the accuracy and precision were deemed suitable, all original pXRF data collected in the field were recalculated. As a result, the following elements were used in data analysis: S, K, Ca, Mn, Fe, Cu, As, Ag, Sb, Hg, and Pb.

5.4. In-field obstacles and adaptations

Although our results were factor corrected and the necessary concentration ranges for each element were covered, with checks made to evaluate accuracy and precision, it is important to note that a variety of other effects still played a role in our analysis in the field. For example, moisture, homogeneity, particle size, mineralogy, and compactness can affect *in situ* pXRF analysis of unprepared soil samples.

Trapiche presented numerous in-field challenges for collecting samples, such as large boulders from rock fall, collapsed walls from historic buildings, and high levels of vegetative ground cover. Some obstacles made pXRF analysis impossible, and we avoided wall-fall to obtain pXRF readings from “natural” ground levels of occupation. Local vegetation included thick stands of ichu grass, which was present inside all structures. Vegetation had to be cleared prior to sampling. Due to these field obstacles, our discussion of the pXRF survey data is best considered to be semi-quantitative only, and we combine the results of the geochemical survey with data from surface architecture to arrive at our interpretations. Further, P (phosphorus) values appear to have been affected by analysis at high altitude, with higher values achieved at high altitude (Puno, Peru) compared with experimental readings conducted in low altitude conditions in both Lima, Peru and Sydney, Australia.

5.5. Data analysis and interpretation

Following factor correction, pXRF values were imported into ArcGIS and spatially mapped with ArcMap. All values were viewed in ppm. We used proportional symbols and colors to represent variation and relied on ArcMap’s natural breaks (jenks) classification method to characterize the data, although in some cases we manually adjusted categories. To identify areas of intense metallurgical activity, we converted each element’s 103 points to a raster with cell size 4, then reclassified on a scale of 0–4, with 0 for no data, 1 for lowest values, and 4 for highest values. The classes were based on natural breaks. The raster values for each element were added together to produce a cumulative raster, which was resampled (bilinear).

Hierarchical cluster analysis was conducted using SYSTAT (v.13.2) software on non-standardized ppm values using complete linkage (farthest neighbor) and the Pearson correlation coefficient (Pearson’s r)

Table 1
Trapiche corrected pXRF values in ppm unless otherwise indicated.

Sector	Survey Location	S	K (%)	Ca (%)	Mn	Fe (%)	Cu	As	Ag	Sb	Hg	Pb
A	0A	897	1.87	1.43	3418	6.05	408	160	127	123	5	1942
A	1A	237	1.89	1.31	2435	6.14	151	60	20	< LOD[1]	10	639
A	2A	253	1.42	1.34	1475	4.03	104	61	38	< LOD	11	592
A	3A	298	1.95	1.90	1500	5.72	95	67	32	31	10	620
A	4A	238	2.04	1.28	1240	6.19	127	55	32	< LOD	12	580
A	5A	202	1.67	1.29	1352	4.56	95	40	26	< LOD	9	557
A	6A	519	1.41	1.20	1852	4.03	126	80	49	< LOD	16	956
A	6B	140	1.63	0.80	886	3.40	88	35	22	< LOD	6	435
A	5B	427	1.81	0.90	1572	4.78	219	90	58	< LOD	28	1121
A	4B	249	1.97	0.94	1294	4.54	131	69	53	< LOD	18	783
A	3B	232	2.08	0.81	1872	4.36	169	77	83	< LOD	21	979
A	2B	146	1.76	0.76	1323	2.99	113	37	48	< LOD	5	626
A	1B	155	1.79	0.89	993	3.20	88	43	24	< LOD	3	473
A	0B	609	1.72	1.21	3666	4.64	541	159	180	90	5	1774
A	0C	< LOD	0.72	0.38	462	1.14	33	27	< LOD	< LOD	< LOD	89
A	1C	< LOD	1.11	0.42	575	1.59	30	26	13	< LOD	< LOD	100
A	2C	< LOD	1.19	0.42	519	1.87	21	25	< LOD	< LOD	< LOD	57
A	3C	< LOD	1.37	0.54	613	1.99	25	24	< LOD	< LOD	< LOD	70
A	4C	< LOD	1.80	0.85	802	2.69	41	31	13	< LOD	< LOD	209
A	5C	192	1.63	1.21	1060	2.75	74	42	34	< LOD	10	494
A	6C	130	1.82	0.73	955	3.33	85	42	23	< LOD	8	450
A	7C	121	1.53	0.75	1017	2.84	58	39	12	< LOD	5	266
A	7D	< LOD	1.81	0.80	859	3.30	45	30	< LOD	< LOD	4	152
A	6D	73	1.79	0.78	969	3.57	44	34	< LOD	< LOD	5	149
A	5D	< LOD	1.51	0.92	783	2.59	43	33	< LOD	< LOD	3	183
A	4D	< LOD	1.31	0.59	796	2.18	27	26	< LOD	< LOD	< LOD	105
A	3D	< LOD	1.29	0.57	820	2.10	23	24	< LOD	< LOD	< LOD	69
A	2D	61	1.50	0.74	749	2.49	26	26	< LOD	< LOD	2	75
A	1D	< LOD	1.91	1.09	763	4.08	32	27	< LOD	< LOD	< LOD	85
A	0D	< LOD	2.18	1.01	1323	3.78	50	36	< LOD	< LOD	3	167
A	mill 3	88	1.54	0.65	1098	2.68	41	33	< LOD	< LOD	< LOD	124
A	mill 2	585	1.19	0.65	4197	3.57	291	636	169	40	25	2024
A	mill 1	145	0.45	0.79	759	0.91	35	< LOD	39	< LOD	< LOD	384
A	SM4	< LOD	2.20	1.14	1898	5.03	284	34	< LOD	< LOD	< LOD	102
A	SM1	4368	2.27	1.31	8091	8.59	800	359	459	223	< LOD	7880
A	horno	976	1.61	0.82	2479	4.21	402	176	147	86	38	2938
A	SM2	11,376	2.70	0.88	11,513	8.21	1547	974	698	635	13	16,397
B	0C	51	0.29	0.43	168	0.75	30	22	14	< LOD	< LOD	99
B	1A	69	0.64	0.45	467	1.18	69	32	12	< LOD	2	219
B	1B	61	1.31	0.75	914	2.50	59	29	13	< LOD	< LOD	169
B	1C	< LOD	1.54	0.70	444	2.75	69	37	13	< LOD	6	244
B	2B	317	1.29	0.63	1431	3.55	177	80	49	25	19	970
B	2C	793	1.83	0.98	1509	5.08	331	153	90	< LOD	43	1726
B	3B	59	1.51	0.99	708	2.98	37	27	17	< LOD	< LOD	107
B	3C	212	1.86	1.00	1156	4.29	141	65	96	32	28	765
B	4B	153	1.23	0.72	650	2.40	38	30	< LOD	< LOD	< LOD	110
B	4C	257	1.64	0.94	1179	3.72	127	68	59	< LOD	63	885
B	5C	626	1.16	0.91	1476	3.17	262	114	103	37	89	1955
B	5B	64	1.52	0.94	694	2.90	28	27	< LOD	< LOD	< LOD	76
B	6C	7240	1.89	1.39	1860	7.09	1287	674	575	291	779	12,201
B	6B	284	1.21	1.12	1077	2.93	144	66	39	< LOD	15	827
B	7B	223	1.40	1.01	746	3.24	915	48	31	< LOD	28	1317
B	7C	459	1.21	1.07	745	2.56	253	55	47	< LOD	23	1538
B	8C	318	1.51	1.07	1155	3.47	206	71	48	< LOD	33	1131
B	8B	403	0.58	1.21	1120	1.37	94	< LOD	44	< LOD	15	603
B	8A	1943	1.48	1.05	1934	4.46	621	273	159	103	361	4681
B	9A	163	1.73	0.80	956	4.30	377	35	14	< LOD	6	982
B	9B	4610	1.66	1.00	3298	7.82	2425	699	291	229	418	9076
B	9C	320	1.30	0.96	658	2.87	316	58	34	< LOD	31	1054
B	10C	1864	1.36	0.87	1848	4.03	995	334	244	62	266	4832
B	10B	645	1.73	1.04	1768	4.81	279	140	82	< LOD	64	1754
B	10A	1312	1.71	1.73	3734	5.31	1408	128	36	55	53	4481
B	11A	422	1.02	0.88	1212	2.32	268	85	54	< LOD	30	1457
B	11B	772	0.99	1.38	2573	2.57	303	81	61	45	38	1652
B	3A	437	1.57	1.08	1366	4.09	275	126	77	41	39	1175
B	5A	370	1.09	0.73	733	2.52	290	91	54	< LOD	27	916
B	9D	< LOD	0.85	0.61	525	1.93	22	22	< LOD	< LOD	< LOD	61
B	10D	< LOD	0.18	0.40	397	0.29	16	19	13	< LOD	< LOD	27
B	11D	< LOD	1.02	0.98	519	2.31	25	25	< LOD	< LOD	< LOD	73
B	8D	< LOD	1.07	0.91	600	2.57	29	25	< LOD	< LOD	< LOD	59
B	7D	84	1.51	1.16	976	3.53	37	28	< LOD	< LOD	3	96
B	7E	< LOD	1.06	0.89	618	2.58	28	25	< LOD	< LOD	< LOD	49
B	5D	< LOD	0.29	0.97	441	0.52	19	19	15	< LOD	< LOD	23
B	3E	169	1.13	0.90	977	3.07	105	47	26	< LOD	62	458

(*continued on next page*)

Table 1 (*continued*)

Sector	Survey Location	S	K (%)	Ca (%)	Mn	Fe (%)	Cu	As	Ag	Sb	Hg	Pb
B	3D	226	0.83	0.69	1198	2.13	79	45	28	< LOD	24	515
C	0A	2041	1.20	0.90	2810	4.92	1339	373	169	214	93	4749
C	0C	11,222	1.80	1.32	7768	11.21	2999	888	225	615	272	10,622
C	0D	10,272	1.67	1.31	5761	7.89	3822	1051	396	583	556	14,923
C	0E	427	0.98	0.99	1187	2.86	167	75	59	23	46	1060
C	1G	81	1.08	0.99	637	2.97	37	28	11	< LOD	< LOD	78
C	1F	68	1.66	1.53	1156	4.26	90	38	25	< LOD	19	506
C	1E	163	1.42	1.20	941	3.59	88	41	34	< LOD	12	543
C	1D	14,565	2.01	1.64	8913	12.06	3302	1245	542	791	698	15,960
C	1C	425	1.34	1.26	1230	3.78	318	94	40	30	28	1110
C	1B no1	1062	1.22	1.18	2864	5.41	791	267	129	128	182	3461
C	1B no2	751	1.11	1.16	1559	4.56	440	237	80	90	31	1785
C	1A	199	0.89	0.80	1060	2.31	247	72	46	< LOD	37	1030
C	2A	1469	1.57	1.05	1210	4.97	610	122	176	156	194	4153
C	2C	233	1.32	1.10	798	3.02	140	33	33	< LOD	21	820
C	2D	258	1.46	1.41	988	4.21	143	62	44	< LOD	22	865
C	2E	430	1.49	1.41	1969	4.36	234	77	81	34	59	1505
C	2F	347	1.56	1.84	1819	6.49	230	76	54	< LOD	57	1045
C	datum	169	1.45	1.39	901	4.35	125	53	32	< LOD	26	651
C	4D	131	1.32	1.02	861	3.28	91	44	26	< LOD	10	361
C	4C	128	0.83	0.65	577	1.86	71	43	24	< LOD	8	353
C	4B	580	0.87	0.75	1340	3.33	332	102	73	39	70	2134
C	4A	111	1.17	0.84	759	2.75	76	37	14	< LOD	10	385
C	3D	892	1.16	0.97	1762	4.42	547	190	87	77	105	2738
C	3C	212	0.67	0.62	478	1.55	120	44	31	< LOD	19	956
C	3B	63	1.31	1.08	856	3.71	58	32	15	< LOD	13	125
N/A	Control 1	130	1.93	2.00	1184	5.74	57	39	< LOD	< LOD	13	165
N/A	Control 2	86	1.79	1.04	1070	5.14	98	46	12	< LOD	9	267
N/A	Control 3	< LOD	2	1	779	3.97	32	27	< LOD	< LOD	4	58

[1] Below "Level of Detection." < LOD values: S (50 ppm), As (3 ppm), Ag (11 ppm), Sb (13 ppm), and Hg (2 ppm).

with a distance metric of 1. It is common to use complete linkage on measurements of chemical elements within samples that have similar baseline composition. Principal component analysis was conducted using Statistica (v.7) and JMP Pro (v.14) software, with data $\log_{10}$ transformed before analysis.

6. Results and discussion

The corrected pXRF results are presented in Table 1.

6.1. Control samples

Three control samples were taken outside of the site boundary to determine a natural soil level baseline for the area (Table 2). Natural soils from the controls included relatively high levels of K, Ca, Mn, and Fe, consistent with normal soil values in this area of the Andes. Sulfur (72 ppm), copper (62 ppm), arsenic (37 ppm), mercury (8 ppm), and lead (163 ppm) averages for the three controls indicate their relatively low levels in natural soils. Chlorine and antimony were below levels of detection in the control samples. Further, of these control samples, Control 3 was taken from the same side of the Itapalluni River as the site, at a higher elevation than the site itself, and has generally lower values of S, Cu, As, Ag, and Hg. The other two controls were taken from the western side of the riverbank and have relatively higher values of the aforementioned elements, possibly due to wind-blown contaminants from the nearby mill.

Table 2
Corrected pXRF values for control samples in ppm unless otherwise indicated.

Element	Control 1	Control 2	Control 3	Average
S	130	86	< LOD[2]	72
Cl[1]	< LOD	< LOD	< LOD	< LOD
K (%)	1.93	1.79	2.11	1.94
Ca (%)	2.00	1.04	0.98	1.34
Mn	1184	1070	779	1011
Fe (%)	5.74	5.14	3.97	4.95
Cu	98	57	32	62
As	46	38	27	37
Ag	< LOD	12	< LOD	4
Sb	< LOD	< LOD	< LOD	< LOD
Hg	12	9	4	8
Pb	165	267	58	163

[1] Chlorine values listed here were not factor corrected.
[2] Below "Level of Detection." < LOD values: S (50 ppm), Cl (n/a), Ag (11 ppm), and Sb (13 ppm).

6.2. Presence of patio process elements

Because prehispanic, indigenous silver smelting technology did not use mercury, we were able to confirm the patio process at Trapiche by the presence of high mercury levels (> 10 ppm) in over 50% of the pXRF samples. We also identified a reverberatory furnace, confirming the Andean technique of roasting ground ore to convert silver sulfides to silver chlorides. Although we were unable to factor correct for chlorine (Cl), an examination of uncorrected Cl concentrations reveals high levels (> 1000 ppm) near the mill and main patio, as well as the reverberatory furnace (369 ppm). These results indicate salt (NaCl) was added during the early roasting stages *and* later amalgamation stages. Further, the combined presence of mercury, salt, and a reverberatory furnace confirm the use of Andean refining techniques at Trapiche.

Relatively high readings of iron (> 110,000 ppm) and copper (> 3000 ppm) were recorded in Sector B's main patio, indicating their probable use for the reduction of silver chloride to elemental silver, also an Andean technique. The distribution of antimony (Sb) at Trapiche was also informative, as Sb only occurs naturally in combination with sulfur, copper, silver, and lead (Anderson, 2012). Sb was present in only 28% of Trapiche samples and was not recorded in any control samples. Sb was identified in the reverberatory furnace (86 ppm), the metallurgical oven (100 ppm), the main patio (> 200 ppm), near the mill (635 ppm), and in Sector C (500–800 ppm) (Fig. 4). Our results indicate that occurrences of Sb at Trapiche are related to processes that separated it from its combined state in ore through grinding or heat.

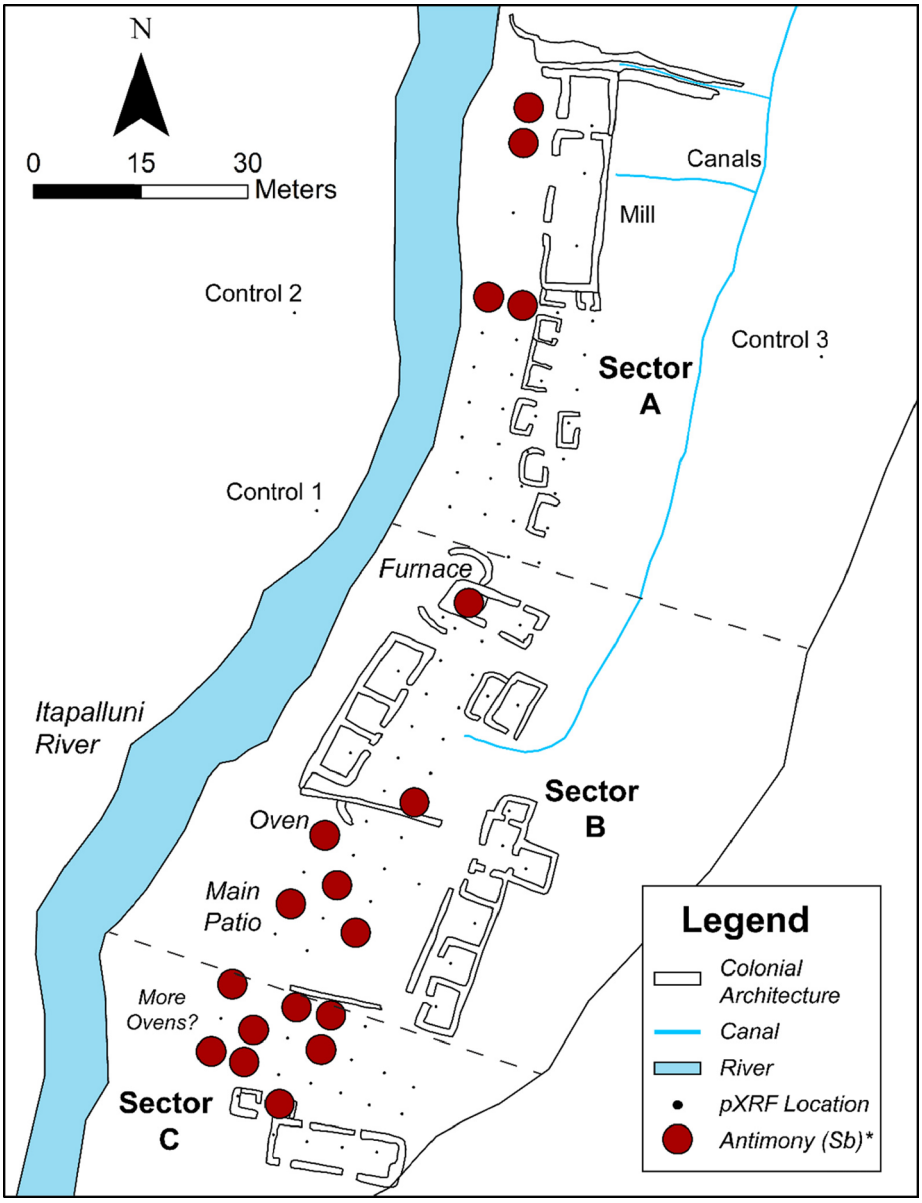

Fig. 4. Location of antimony (Sb) at Trapiche. *Sb readings are > 50 ppm.

6.3. Distribution and correlation of elements

To spatially visualize zones of intense metallurgical activity, we created a cumulative raster from pXRF values (Fig. 5). Three high-intensity metallurgical areas were identified. These corresponded to the mill, the main patio, and Sector C. Locations with little or no metallurgical activity corresponded to domestic structures. The highest levels of mercury (Hg) (> 500 ppm) were recorded near the metallurgical oven in Sector B. This confirms the evaporation and collection of Hg in this area. Further, *pellas* were washed in tanks and canals directly north of the oven, also likely contributing to higher levels of Hg in this zone. The main patio in Sector B was another area of intense metallurgical activity and was the likely location where various agents, such as copper sulfate and iron, were mixed with silver ore in heated *buitrones*. The highest readings of S (14,565 ppm), Sb (791 ppm), Fe (120,631 ppm), and Cu (3822 ppm) occurred directly south and downhill of the main patio. We interpret these high values in Sector C as the result of runoff. However, we cannot eliminate the possibility that Sector C was used for amalgamation processes.

Hierarchical cluster analysis with complete linkage was used to compare and group similar elemental values and is represented in a dendrogram (Fig. 6). The most similar elements clustered first, on the far-left of the graph. Sulfur and antimony grouped together for the first linkage, indicative of their closely combined state in nature (Anderson, 2012). They also group with silver in the first cluster, likely representative of silver sulfide ore, such as argentite (Ag_2S), mined in the Puno Bay (Schultze, 2008). Arsenic, copper, and lead also form an early cluster. This may indicate use of a lead ore combined with copper, silver, and antimony, possibly in pyrite, sphalerite, or barite. However, galena (PbS) has also been identified as a common Puno Bay lead source (Schultze, 2008). Perhaps the arsenic, copper, and lead cluster indicate the composition of copper ore brought to Trapiche for use in the *magistral*.

Mercury and iron also join the arsenic, copper, and lead cluster, although many linkages later. In fact, mercury is one of the very last elements to join a cluster during the hierarchical cluster analysis. This highlights mercury's unique use and importance as it was added to multiple stages of the patio process. It also highlights how ubiquitous

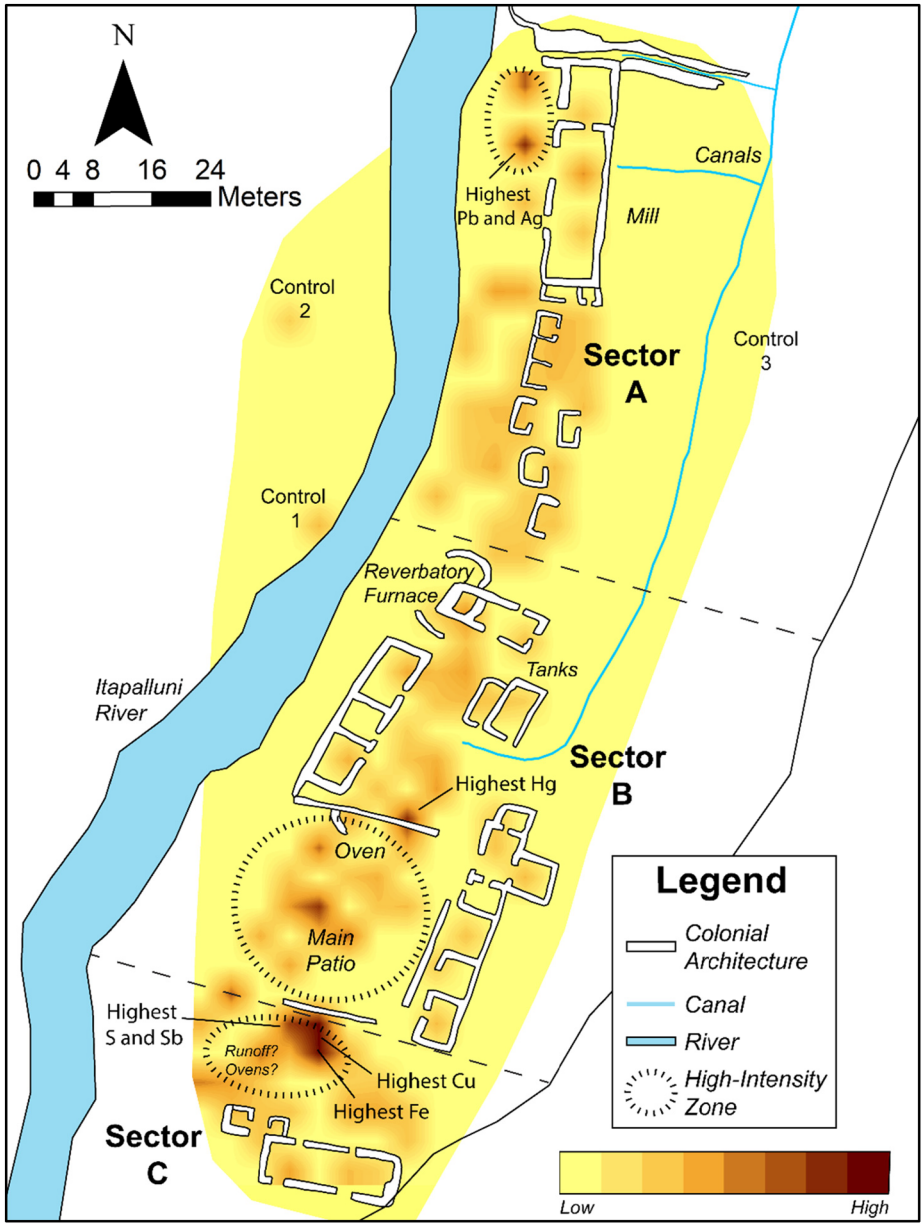

Fig. 5. Trapiche cumulative raster depicting zones of intense metallurgical activity.

mercury was at the site (in 75% of all samples). Calcium and potassium form the final cluster of the analysis and represent natural elements present in soils throughout the site.

Principal component analysis was conducted to evaluate potential groupings of survey locations by elemental concentrations across the site. The first three principal components accounted for over 90% of the variation in the sample population. Many samples taken from Sector A, as well as some from Sector B, form a group. They are distinguished from the remainder of the locations due to higher K and Ca values and relatively lower amounts of Hg, Pb, As, Cu, S, Ag, and Sb. These results are consistent with areas of the site not being used for intensive metallurgical activities in comparison with the remainder of Trapiche. This group includes locations outside of the mill area in Sector A, apart from one mill building sample, buildings in both Sectors A and B, and some patio areas of Sector B. In some cases, this association might be due to failing to reach the 'natural ground' due to rock fall and rubble, particularly in some areas of Sector B where higher amounts of mercury might be expected.

Other locations at Trapiche had relatively high amounts of Pb, As, Cu, S, Ag, and Sb, correlating with grinding activities, and to a lesser extent run-off from canals. Group associations with relatively higher amounts of mercury were found in the main patio, the reverberatory furnace, and Sector C. The high values of mercury in Sector C correlate with the area in front of the multipurpose building, noted earlier as related to run-off from the main patio, as well as a small structure which may have been used as storage for silver and mercury. Descriptions of refining mills from this period indicate guarded warehouses of mercury near the principal entrance (Arzáns de Orsúa y Vela, 1965). The lack of Sector A group associations with mercury suggests that mercury was likely imported to Trapiche in its final form to be

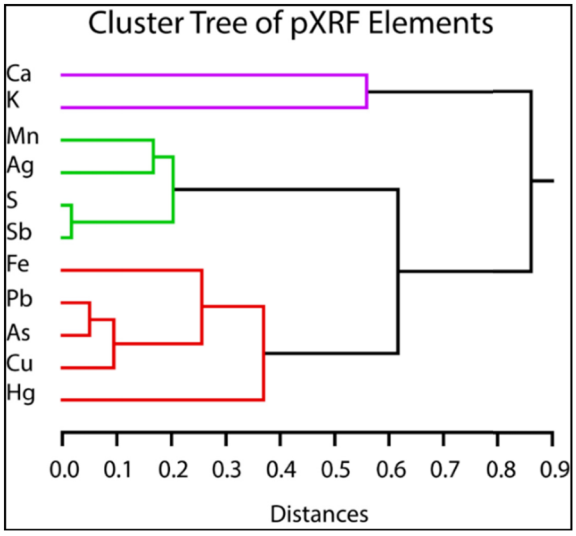

Fig. 6. Dendrogram with complete linkage clustering.

added in the amalgamation stages and was not involved in ore grinding or processing.

7. Conclusion

This study identified the use of the patio process silver refining technique at Trapiche Itapalluni, a colonial period silver refinery located in the western Lake Titicaca Basin of Peru (1650–1800 CE). Using a pXRF spectrometer, we conducted a site-level soil survey and identified high levels of mercury, copper, and sulfur, confirming the use of mercury amalgamation and copper sulfate during the patio process of silver refinement. We also identified multiple local, Andean adaptations to the patio process, such as roasting ore, adding heat during amalgamation, and using copper and iron to reduce silver chloride to elemental silver. Finally, our pXRF survey revealed that P was affected by high-altitude in the field. Our study shows the applicability and feasibility of using pXRF technology for geochemical site prospection in archeometallurgical sites in the Andes and other high-altitude, marginal environments.

Declaration of Competing Interest

The authors declare that they have no known competing financial interests or personal relationships that could have appeared to influence the work reported in this paper.

Acknowledgements

Research was funded by a Wenner-Gren Foundation Dissertation Fieldwork Grant (#9605), as well as a University of New South Wales (UNSW) Mark Wainwright Analytical Centre (MWAC) Research Grant. Thank you to the MWAC at UNSW for lending field equipment, as well as for providing space to prepare and run our samples. Thank you also to Rabeya Akter from the ICP Laboratory, MWAC, for analyzing our samples for Hg. Research by the Proyecto Arqueológico con Excavaciones Trapiche (PAT) was authorized by the Peruvian Ministry of Culture with the following permit: RDN 337-2018/DBPA/VMPCIC/MC (2018). Karen Durand Caceres and Jorge Rosas Fernandez were codirectors of the project in 2018 and 2019. The CARI field house in Puno lent equipment, laboratory, and storage space and Javier Chalcha Saraza, Oliver Quispe, Felipa Aroqutipa, Julia Sjodahl, and Courtney Besaw assisted on the pXRF survey. We thank Aubrey Hillman for her insightful comments on a draft of this manuscript, as well as the helpful comments from two anonymous reviewers. This article was written during Kennedy's Junior Fellowship in Pre-Columbian Studies at Dumbarton Oaks Research Library and Collection.

References

Abbott, M.B., Wolfe, A.P., 2003. Intensive pre-incan metallurgy recorded by lake sediments from the bolivian andes. Science 301, 1893. https://doi.org/10.1126/science.1087806.

Aimers, J.J., Farthing, D.J., Shugar, A.N., 2012. Handheld XRF analysis of Maya ceramics: A pilot study presenting issues related to quantification and calibration. Handheld XRF Art Archaeol. 423–448.

Anderson, C.G., 2012. The metallurgy of antimony. Interdisciplinary J. Chem. Prob. Geosci. Geoecol. 72, 3–8.

Arzáns de Orsúa y Vela, 1965. Bartolomé et al. Historia De La Villa Imperial De Potosí. Edited by Hanke and Mendoza. Brown University Bicentennial Publications. Brown University Press, Providence, RI.

Barba, A.A., 1640... *Arte de los metales.* Goldsmiths'-Kress library of economic literature. En la imprenta del reyno no. 701.

Bargalló, M., 1969. La amalgamación de los minerales de plata en hispanoamérica colonial. Compañía Fundidora de Fierro y Acero de Monterrey, México, D.F.

Bargalló, M., 1966. La química inorgánica y el beneficio de los metales en el México prehispánico y colonial, Primera edición. ed, Química en México ; tomo 1. Universidad Nacional Autónoma de México, México.

Bigelow, A.M., 2020. Mining language: Racial thinking, indigenous knowledge, and colonial metallurgy in the early modern iberian world. UNC Press/OIEAHC.

Booth, A.D., Vandeginste, V., Pike, D., Abbey, R., Clark, R.A., Green, C.M., Howland, N., 2017. Geochemical insight during archaeological geophysical exploration through in situ X-ray fluorescence spectrometry. Archaeol. Prospect. 24, 361–372. https://doi.org/10.1002/arp.1575.

Guía y histórica, geográfica, física, política, (Ed.), 1952. civil y legal del Gobierno e Intendencia de la Provincia de Potosí, Colección de la cultura boliviana. Colección primera; Los escritores de la colonia no. 1 Editorial Potosí, Potosí.

Cooke, C.A., Abbott, M.B., Wolfe, A.P., 2008. Late-holocene atmospheric lead deposition in the peruvian and bolivian andes. Holocene 18, 353–359. https://doi.org/10.1177/0959683607085134.

Coronel, E.G., Bair, D.A., Brown, C.T., Terry, R.E., 2014. Utility and limitations of portable X-Ray fluorescence and field laboratory conditions on the geochemical analysis of soils and floors at areas of known human activities. Soil Sci. 179.

Dodge, M.D., 1984. Silver mining and social conflict in seventeenth-century Peru: the war of the nations in Laicacota, 1665-1667. ProQuest Dissertations Publishing.

Dominguez, N.J., 2006. Rebels of Laicacota: Spaniards, Indians, and Andean mestizos in southern Peru during the mid -colonial crisis of 1650–1680. ProQuest Dissertations Publishing.

ESDAC (European Soil Data Centre (ESDAC)., 2020. Join Research Center European Social Data Centre.

Frahm, E., Monnier, G.F., Jelinski, N.A., Fleming, E.P., Barber, B.L., Lambon, J.B., 2016. Chemical soil surveys at the Bremer Site (Dakota county, Minnesota, USA): Measuring phosphorous content of sediment by portable XRF and ICP-OES. J. Archaeol. Sci. 75, 115–138. https://doi.org/10.1016/j.jas.2016.10.004.

Galaor, I., 1998. Las minas hispanoamericanas a mediados del siglo XVIII: informes enviados al Real Gabinete de Historia Natural de Madrid. Iberoamericana, Madrid.

Guerrero, S., 2016. The history of silver refining in New Spain, 16c to 18c: back to the basics. History Technol. 32, 2–32. https://doi.org/10.1080/07341512.2016.1191864.

Guerrero, Saul, 2017. Silver by fire, silver by mercury: A chemical history of silver refining in New Spain and Mexico, 16th to 19th Centuries. BRILL, Boston. https://doi.org/10.1163/9789004343832.

Hanks, B., 2013. Notes from the field. IANSA 1 (4), 3–5.

Hayes, K., 2013. Parameters in the use of pXRF for archaeological site prospection: A case study at the Reaume Fort Site, Central Minnesota. J. Archaeol. Sci. 40, 3193–3211. https://doi.org/10.1016/j.jas.2013.04.008.

Hunt, A.M., Speakman, R.J., 2015. Portable XRF analysis of archaeological sediments and ceramics. J. Archaeol. Sci. 53, 626–638.

Jones, G., 2001. Geophysical investigation at the falling creek ironworks, an early industrial site in Virginia. Archaeol. Prospect. 8, 247–256. https://doi.org/10.1002/arp.173.

Killick, D., 2015. The awkward adolescence of archaeological science. J. Archaeol. Sci. 56, 242–247.

Kincey, M., Warburton, J., Brewer, P., 2018. Contaminated sediment flux from eroding abandoned historical metal mines: Spatial and temporal variability in geomorphological drivers. Geomorphology 319, 199–215. https://doi.org/10.1016/j.geomorph.2018.07.026.

Lubos, C., Dreibrodt, S., Bahr, A., 2016. Analysing spatio-temporal patterns of archaeological soils and sediments by comparing pXRF and different ICP-OES extraction methods. J. Archaeolog. Sci.: Rep. 9, 44–53. https://doi.org/10.1016/j.jasrep.2016.06.037.

MacKenzie, A.B., Pulford, I.D., 2002. Investigation of contaminant metal dispersal from a disused mine site at Tyndrum, Scotland, using concentration gradients and stable Pb isotope ratios. Appl. Geochem. 17, 1093–1103. https://doi.org/10.1016/S0883-2927(02)00007-0.

Malainey, M.E., 2011. A Consumer's Guide to Archaeological Science: Analytical Techniques, Manuals in Archaeological Method. Theory and Technique, Springer,

New York, New York, NY.
Merrill, J., Montenegro, V., Gazley, M.F., Voisin, L., 2018. The effects of pressure on X-ray fluorescence analyses: pXRF under high altitude conditions. J. Anal. At. Spectrom. 33, 792–798.
Millard, A.R., 1999. Geochemistry and the early alum industry. Geol. Soc. London, Special Publ. 165, 139. https://doi.org/10.1144/GSL.SP.1999.165.01.10.
Padilla, J.R., Hormes, J., Selim, H.M., 2019. Use of portable XRF: Effect of thickness and antecedent moisture of soils on measured concentration of trace elements. Geoderma 337, 143–149.
Rogan, G., Tighe, M., Grave, P., Kealhofer, L., Yukongdi, P., Wilson, S.C., 2019. Optimization of portable X-ray fluorescence spectrometry for the assessment of soil total copper concentrations: application at an ancient smelting site. J. Soils Sediments 19, 830–839. https://doi.org/10.1007/s11368-018-2091-3.
Robins, Nicholas A., 2011. Mercury, Mining, and Empire: The human and Ecological cost of Colonial Silver Mining in the Andes. Indiana University Press.
Robins, Nicholas A., Hagan, Nicole A., 2012. Mercury production and use in colonial Andean silver production: emissions and health implications. Environ. Health Perspect. 120, 627–631.
Schultze, C.A., 2013. Silver Mines of the Northern Lake Titicaca Basin. In: Tripcevich, N., Vaughn, K.J. (Eds.), Mining and Quarrying in the Ancient Andes: Sociopolitical, Economic, and Symbolic Dimensions, Interdisciplinary Contributions to Archaeology. Springer, New York, NY, pp. 231–251. https://doi.org/10.1007/978-1-4614-5200-3_11.
Schultze, C.A., 2008. The Role of Silver Ore Reduction in Tiwanaku State Expansion into Puno Bay. University of California, Los Angeles, Peru.
Scott, R.B., Eekelers, K., Degryse, P., 2016. Quantitative chemical analysis of archaeological slag material using handheld X-ray fluorescence spectrometry. Appl. Spectrosc. 70, 94–109. https://doi.org/10.1177/0003702815616741.
Shackley, M.S., 2011. An introduction to X-ray fluorescence (XRF) analysis in archaeology, in: *X-Ray Fluorescence Spectrometry (XRF)*. In: Geoarchaeology. Springer, pp. 7–44.
Shackley, M.S., 2010. Is there reliability and validity in portable X-ray fluorescence spectrometry (PXRF). SAA Archaeol. Record. 10, 17–20.
Shalev, S., Shilstein, S.S., Yekutieli, Y., 2006. XRF study of archaeological and metallurgical material from an ancient copper-smelting site near Ein-Yahav, Israel. Talanta 70, 909–913. https://doi.org/10.1016/j.talanta.2006.05.052.
Speakman, R.J., Little, N.C., Creel, D., Miller, M.R., Iñañez, J.G., 2011. Sourcing ceramics with portable XRF spectrometers? A comparison with INAA using Mimbres pottery from the American Southwest. J. Archaeol. Sci. 38, 3483–3496.
Speakman, R.J., Shackley, M.S., 2013. Silo science and portable XRF in archaeology: A response to Frahm. J. Archaeol. Sci. 40, 1435–1443.
Tighe, M., Rogan, G., Wilson, S.C., Grave, P., Kealhofer, L., Yukongdi, P., 2018. The potential for portable X-ray fluorescence determination of soil copper at ancient metallurgy sites, and considerations beyond measurements of total concentrations. J. Environ. Manage. 206, 373–382. https://doi.org/10.1016/j.jenvman.2017.10.052.
USGS (United States Geological Survey), 2020. MRData Global. Mineral Resources. Online.
Van Buren, M., Mills, B.H., 2005. Huayrachinas and tocochimbos: Traditional smelting technology of the southern Andes. Latin Am. Antiquity 16, 3–25. https://doi.org/10.2307/30042484.
Van Buren, M., Cohen, C.R., 2010. Technological changes in silver production after the spanish conquest in Porco, Bolivia. Boletín del Museo Chileno de Arte Precolombino 15, 29–46. https://doi.org/10.4067/S0718-68942010000200003.
White, H., Dungworth, D., 2007. Warmley Brassworks. Analysis of Some Eighteenth-century Brassworking Debris. English Heritage, Siston, Bristol.